Climate Services 42 (2026) 100636

Contents lists available at ScienceDirect

Climate Services

journal homepage: www.elsevier.com/locate/cliser

Original research article

A framework for generating catalogues of high-impact UNSEEN flood events

Elena Bianco [a,1], Paolo Davini [b], Giuseppe Zappa [c], Agostino Manzato [c,2], Antonio Giordani [a,d], Paolo Ruggieri [a,*]

[a] Dipartimento di Fisica e Astronomia "Augusto Righi", University of Bologna, Bologna, Italy
[b] Istituto di Scienze dell'Atmosfera e del Clima, Consiglio Nazionale delle Ricerche (CNR-ISAC), Torino, Italy
[c] Istituto di Scienze dell'Atmosfera e del Clima, Consiglio Nazionale delle Ricerche (CNR-ISAC), Bologna, Italy
[d] ItaliaMeteo - National Agency for Meteorology and Climate, Bologna, Italy

ARTICLE INFO

Dataset link: https://zenodo.org/records/18260378, 10.5281/zenodo.18260378, https://ewds.climate.copernicus.eu/datasets/efas-historical?tab=download, https://ewds.climate.copernicus.eu/datasets/efas-reforecast?tab=download, https://cds.climate.copernicus.eu/datasets/seasonal-original-single-levels?tab=download, https://cds.climate.copernicus.eu/datasets/seasonal-original-pressure-levels?tab=download, https://www.ecmwf.int/en/forecasts/dataset/ecmwf-reanalysis-v5, https://climada-python.readthedocs.io/en/stable/, https://www.hydrosheds.org/products/hydrobasins

Keywords:
Flood extremes
Ensemble prediction
Impact modelling
Risk framework

ABSTRACT

In recent years, Europe has experienced several episodes of catastrophic flooding that were unprecedented in the historical record. Estimating the impact of rare flood events is crucial for improving risk preparedness and emergency management, but this effort is hampered by the limited availability of historical data. We describe a modular framework for generating a catalogue of physically plausible high-impact flood events using ensemble prediction systems. The framework builds on existing methodologies for the analysis, validation, and pooling of seasonal reforecasts from the European Flood Awareness System (EFAS) with the UNSEEN (UNprecedented Simulated Extremes using ENsembles) approach. We employ the probabilistic impact model CLImate ADAptation (CLIMADA, Aznar-Siguan and Bresch (2019)) to identify a subset of events with severe impact potential. Synoptic patterns are reconstructed using the ECMWF SEASonal forecasts version 5 (SEAS5) reforecasts to form a catalogue of plausible extremes. We illustrate the case study of the Panaro watershed in Emilia-Romagna, Italy, a region affected by multiple record-breaking floods in recent years. The analysis illustrates the added value of combining ensemble pooling with impact modelling, to anticipate high-impact extreme events before they occur. Our framework can be leveraged to explore risk storylines for stress-testing, and to support adaptation decision making for disaster management.

Practical implications

Every year, hydro-meteorological extremes cause extensive socio-economic damage worldwide, with a substantial number of flood hazards occurring over the European territory. Actionable information on the frequency and characteristics of extreme events is essential for evaluating the effectiveness of flood-mitigation and adaptation strategies. While the need to develop robust local adaptation measures is widely recognized, aleatoric and epistemic uncertainty arising from the large internal variability of the climate system and the complexity of flood drivers pose significant challenges to forecasters and policy-makers. Furthermore, assessing the frequency of severe flood events, such as those with return periods higher than 100 years, is fundamentally hampered by the limited length of the historical record. Observations typically provide only a few episodic examples of severe floods for a given region — an insufficient amount of data to statistically infer the frequency and consequently assess the risk of these events.

Continued advances in ensemble weather and climate forecasting, including refined spatial resolutions and skillful predictions over the Euro-Atlantic region, have enabled the application of ensemble prediction systems to explore a much wider range of past and present weather extremes. This approach, pioneered by Osinski et al. (2016) and also known as UNprecedented Simulated Extreme using ENsembles (UNSEEN, Thompson et al. 2017), consists of treating individual ensemble members of a weather prediction model as equally plausible alternatives to the observed evolution of a given system, providing large quantities of physically-realistic events that may have not been observed yet.

In this study, we build on the UNSEEN approach and established methodologies for flood risk assessment to generate catalogues of

* Correspondence to: Dipartimento di Fisica e Astronomia "Augusto Righi", University of Bologna, 40126, Bologna Italy.
E-mail addresses: elena.bianco3@unibo.it (E. Bianco), paolo.ruggieri2@unibo.it (P. Ruggieri).
[1] Current affiliation: School of Geography, Earth and Environmental Sciences, University of Birmingham, Birmingham, United Kingdom.
[2] Current affiliation: ARPA FVG - OSMER, Palmanova (UD), Italy.

https://doi.org/10.1016/j.cliser.2026.100636
Received 26 September 2025; Received in revised form 16 January 2026; Accepted 17 January 2026
Available online 23 January 2026

physically plausible yet unrealized flood extremes with high potential for socio-economic damage. We describe an end-to-end framework with three flexible modules, (i) ensemble pooling of simulated extremes, (ii) risk assessment with the open-source impact model CLIMADA, and (iii) creation of a catalogue for plausible flood events. The final catalogue incorporates a subset of events that would cause severe economic damage, as well as the synoptic preconditioning drivers of such events. The framework is fully enabled by open-source data provided by the Copernicus Services, and can be adapted to study any European region with sufficient data coverage and validation skill. We demonstrate the application of the framework on a medium-sized European watershed by illustrating the case study of the Panaro river in Emilia-Romagna, Italy, a region that has experienced unprecedented floods in recent years. The region additionally represents an area with ongoing adaptation planning and active stakeholder participation, an ideal setting for the evaluation of existing and innovative risk management strategies. Our framework helps to navigate uncertainty by identifying physically plausible extreme flood events, understanding their preconditioning synoptic drivers, and exploring the possible socio-economic impact of their occurrence at the regional scale. By exploring hypothetical extreme events that might cause severe stress to a given region, policymakers could develop ex-ante mitigation strategies to reduce the impacts of these events before they occur.

1. Introduction

In recent years, Europe has experienced several episodes of extreme flooding. More than 200 deaths are estimated to have occurred in Europe during the summer 2021 floods that affected parts of Germany and the Benelux countries (Merz et al., 2024; Mohr et al., 2022; Tradowsky et al., 2023). In May 2023, the Emilia-Romagna region in Italy was affected by extreme precipitation leading to extensive flooding and over 65,000 landslides (Brath et al., 2023; Marchi et al., 2025). This event was unprecedented in the 102-year instrumental history of the region (Brath et al., 2023; Dorrington et al., 2024). More than 20 people died as a result of the floods that affected Central Europe in September 2024 (Kimutai et al., 2024) and over 200 deaths occurred in Valencia in October 2024 (Llasat, 2024), during what marked the deadliest natural disaster in Spain since 1973. These exceptional events have few, if any, direct historical precedents (Aon Impact Forecasting, 2024; Rhein and Kreibich, 2025).

In several regions of the world, including parts of Europe, an increase in the occurrence of 100-year return periods has been observed (Blöschl et al., 2019), highlighting a regional shift towards a higher frequency of rare flood events. Estimating the intensity and frequency of these exceptional events is crucial for adaptation decision making, as disastrous impacts typically occur with hazard intensities associated with high return periods. However, modelling the tail of the extreme distribution requires volumes of data that are typically unavailable given the brevity of historical records. The limited availability of observational time series prevents robust statistical analysis of low likelihood events, such as those with return periods greater than 100 years, often leading to a systematic underestimation of extreme events (Zeder et al., 2023). As a result, when rare events occur, they are unprecedented or perceived as unprecedented (Merz et al., 2024) and are met by society and policy makers with both surprise and underpreparedness.

Recent advances in climate science have led to the development of new approaches to address unprecedented extremes (Kelder et al., 2025). For example, stochastic weather generators have been used to increase the sample size by statistically emulating observed extremes (e.g., Furrer and Katz, 2008; Winter et al., 2020). However, these methods come with limited physical realism because of the difficulty of capturing the processes and interactions that underscore weather-related hazards: for instance, while there is a theoretical expectation that flood occurrences increase in response to heavier precipitation (e.g., Donat et al., 2016), this relationship is complicated by the complexity of flood drivers (Sharma et al., 2021; Wasko and Nathan, 2019), often involving the occurrence of multiple concurrent factors — the so-called compound floods (e.g., Zscheischler et al., 2018).

To address this issue, ensemble prediction systems (EPS) represent a valuable tool for quantifying the likelihood of severe extremes, as unrealized events from ensemble retrospective forecasts can be pooled to increase the event sample size allowing for robust extreme event analysis (Van den Brink et al., 2004). The core goal of this approach – known as UNprecedented Simulated Extreme using ENsembles (UNSEEN, Thompson et al. 2017, 2019) – is to use a large ensemble of initialized weather model simulations to construct a physically consistent set of plausible extremes, treating EPS members as feasible alternative realizations of the historical period. Thompson et al. (2017) first demonstrated that the UNSEEN approach could be effectively used to anticipate the 2013/2014 UK floods, despite such event did not have any historical precedent in the available record.

Brunner and Slater (2022) used retrospective forecasts from the European Flood Awareness System (EFAS) to pool simulated flood events into an ensemble of 130 timeseries, finding on average a reduction of ~80% in the uncertainty bounds with respect to observational estimates in 200 European river basins. Klehmet et al. (2024) demonstrated the advantage of constructing surrogate time series from the European Centre for Medium-Range Weather Forecasts (ECMWF) SEASonal forecasts version 5 (SEAS5) reforecasts to reduce the uncertainty of return period estimates for precipitation and discharge. Besides flood risk, EPS have been leveraged to improve the quantification of rare extremes across a wide range of applications, including heavy precipitation (e.g., Kelder et al., 2020; Kent et al., 2022; Lang and Poschlod, 2024; Poschlod et al., 2020), tropical cyclones and windstorms (Osinski et al., 2016; Ng and Leckebusch, 2021), wildfires (Sauer et al., 2021), droughts (Chan et al., 2024; Kent et al., 2017, 2019; Pascale et al., 2020), and heatwaves (Fischer et al., 2023; Kelder et al., 2022a).

A major advantage of ensemble pooling is that it enables the development of storylines (e.g., Zappa and Shepherd, 2017; Schaller et al., 2020; Sillmann et al., 2021; Chan et al., 2022; Thompson et al., 2025), defined as plausible, self-consistent unfoldings of past events (Shepherd et al., 2018). This includes using remarkable historical events as a reference to assess new hypothetical scenarios, or downward counterfactuals (Woo, 2019; Ciullo et al., 2021; Merz et al., 2024), whereby the risk arising from small variations in the preconditioning factors leading to the observed hazard is quantified to examine historical 'near misses' and avoid surprises in future catastrophes (Woo, 2019; Curipoma-Viteria et al., 2023).

Ultimately, the goal of exploring unrealized but physically-plausible extreme events is to support the development of effective adaptation plans to mitigate the impact of catastrophic disasters before they occur. Making informed decisions about adaptation requires a careful evaluation of the factors that cause certain extreme events to be more catastrophic than others. This translates into the need for a comprehensive quantification of risk that is not limited to the hazard, but includes information on local asset exposure and vulnerability, consistent with the Intergovernamental Panel on Climate Change (IPCC) definition of risk (IPCC, 2012). One of the most flexible publicly available software for impact modelling is CLIMate ADAptation (CLIMADA, Aznar-Siguan and Bresch 2019. CLIMADA is a modular and object-oriented platform for probabilistic risk assessment of natural hazards. An important advantage of CLIMADA is the highly customizable software structure, which has enabled its application to different types of meteorological extremes, including tropical cyclones (e.g., Eberenz et al., 2021), windstorms (e.g., Walz and Leckebusch, 2019; Röösli et al., 2021), and floods (Sauer et al., 2021; Kam et al., 2025).

Building on existing methodologies, we present an end-to-end framework for generating a catalogue of unprecedented flood events with high impact potential. Physically self-consistent but unrealized (UNSEEN) extreme discharge events are first identified using the EFAS river discharge ensemble seasonal reforecast forced by SEAS5 (EFAS5). The

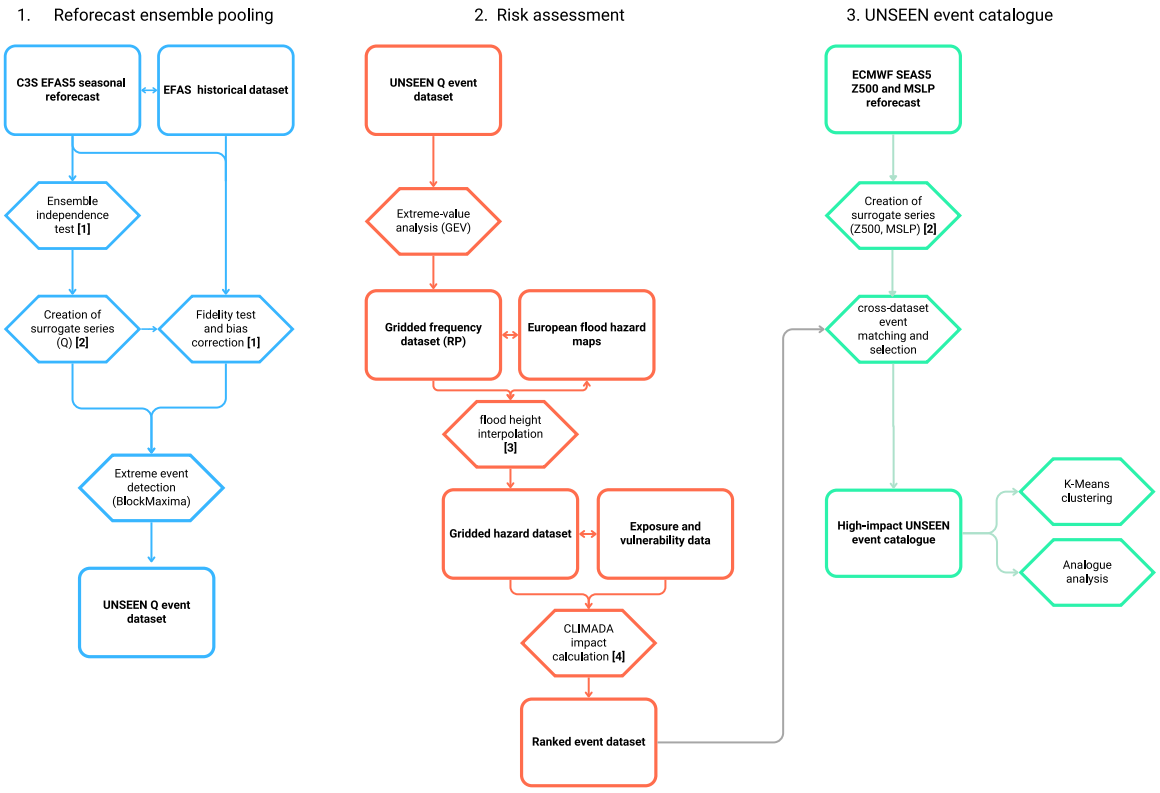

Fig. 1. Schematic of the framework with its three module components. Hexagons indicate processes; rectangles indicate input and output datasets. Indexing refers to published methodologies that are integrated in the framework: **[1]** Kelder et al. (2022a) and references therein; **[2]** Klehmet et al. (2024); **[3]** Riedel et al. (2024); **[4]** Aznar-Siguan and Bresch (2019).

risk model CLIMADA is then used to identify UNSEEN events associated with high economic damage. The synoptic characteristics of selected events are evaluated, to support the construction of a catalogue of plausible, high impact meteorological events. The resulting event set provides a robust physical foundation for exploring realistic worst-case scenarios and supporting preparedness to disastrous events at the regional level. Building on its modular design, the framework can be tailored to suit regions with different sizes and data characteristics.

The remainder of the paper is organized as follows: Section 2 describes the framework, which is structured in three flexible and adaptable modules. The methodology for validating and pooling the EFAS5 seasonal reforecast (Module 1) is outlined in Section 2.3. Flood risk assessment, including the application of CLIMADA for impact modelling (Module 2), is described in Section 2.4. The approach for generating the final event catalogue (Module 3) using the SEAS5 seasonal reforecast is summarized in Section 2.5. In Section 3, we illustrate the application of the framework with a case study in Emilia-Romagna, Italy. Finally, the implications and limitations of the study are discussed and summarized in Section 4.

2. Data and methods

2.1. The framework

The schematic presented in Fig. 1 summarizes the proposed framework with its three modules: (i) reforecast ensemble pooling and validation, (ii) event impact estimation with CLIMADA, and (iii) construction of the UNSEEN event catalogue. Within the framework, state-of-the-art statistical techniques for extreme event analysis are integrated and combined in a unified modelling chain, where the EFAS5 and SEAS5 ensemble reforecasts are used as input data and the catalogue of plausible high impact floods is the final output. The datasets and methodologies composing the framework are presented in detail in the following sections.

2.2. Datasets

2.2.1. EFAS historical and seasonal reforecast

Historical river discharge (Q) is derived from the EFAS v5.0 dataset at 6-hourly intervals and averaged to daily-mean values. EFAS historical data are produced by forcing the LISFLOOD model with gridded precipitation and temperature observations from the European Meteorological Observations version 1 (EMO1, Thiemig et al. 2022) at a resolution of 1x1 arcminute. We note that while gauge measurements of river discharge for our case study region are available from ARPA Emilia Romagna (www.arpae.it; last access: January 2026), this observational source was not included in our analysis due to temporal gaps in the data and the introduction of flood detention basins in 1985 (Figure S1).

We derive seasonal reforecasts of daily river discharge from EFAS5 (Thielen et al., 2009). EFAS reforecasts provide probabilistic medium-range forecasts of river discharge and other key hydrological variables by combining ensemble seasonal meteorological forecasts from ECMWF SEAS5 with the hydrological model LISFLOOD (Van Der Knijff et al., 2010) at a gridded horizontal resolution of 1 × 1 arcminute. The ensemble consists of 25 ensemble members up until December 2016, and 51 members from 2017. Simulations are initialized once a month and extend for a lead time of 215 days (approximately 7 months). We consider the 25-member ensemble simulations for all initialization months and lead times. Although EFAS historical and reforecast data are available from January 1991, we only consider the period between 1999 and 2024 due to a warm SST bias in the North Atlantic in the SEAS5 product before this period (Stockdale et al., 2018). The EFAS data sets extend throughout the European domain. In our case study

analysis (Section 3), the target basin is extracted by masking the data with vectorized polygon layers provided in the HydroBASINS dataset of HydroSHEDS (Lehner et al., 2008), which includes nested boundaries of river basins and sub-basins at different scales with a full global coverage.

2.2.2. SEAS5 seasonal reforecast

Mean sea level pressure (MSLP) and geopotential height at 500hPa (Z500) are obtained from the ECMWF SEAS5 seasonal reforecast for the region between 30°N–70°N and 40°W–40°E. The atmospheric component of SEAS5 is the ECMWF Integrated Forecasting System (IFS) 34r1, with 91 vertical levels. Initialization comes from ERA-Interim reanalysis (ERA-I) up to 2016 and from the ECMWF operational analysis after 2017. As for EFAS reforecasts, we consider the 25-member ensemble for all available initialization dates between 1999–2024. Historical MSLP and Z500 fields between 1999–2024 are obtained from the ECMWF ERA5 reanalysis (Hersbach et al., 2020) for the same domain.

2.3. Module 1: Reforecast ensemble pooling

2.3.1. Statistical independence of the reforecast ensemble

Using reforecast simulations to maximize the sample size of weather extremes relies on the assumption that the individual members of the ensemble are physically and statistically independent (e.g., Van den Brink et al., 2004). Ensemble members must be treated as equally plausible realizations of the past for a given physical system (Kelder et al., 2022a), such that their pooling does not artificially inflate the sample size without adding any new information. While ensemble independence is inherently low at short lead times (e.g. <15 days), members are expected to decorrelate as stochastic processes in the atmosphere drive their trajectories to diverge away from their initial states. The predictability scales of meteorological variables can vary from a few days to a few months. For example, Kelder et al. (2022b) found that member independence for precipitation extremes in SEAS5 reforecasts is achieved within less than a few weeks. For river discharge, ensemble independence is tightly linked to the catchment's seasonality regime (Brunner and Slater, 2022), and is generally achieved at longer lead times compared to atmospheric variables (Klehmet et al., 2024). To robustly assess the independence among the members of the ensemble, we initially calculate the pairwise Spearman rank correlation coefficient (ρ) between the members. In particular, we perform this analysis for a representative location in the target region, which we identify as the grid cell closest to the river hydrometric station, after ensuring that the spatial correlation between the reference grid point and the other grid points along the river is high (>0.9). We first select the maximum discharge during the full 215-day forecast period (F_{max}) for each available starting date between 1999 and 2024. Secondly, we arrange F_{max} values into 12 matrices, each for a different initialization month, so that each matrix contains a time series of F_{max} values for the 25 members of the ensemble. We compute the pairwise ρ between the 25 members for each initialization month and test whether the mean ρ is significantly different from zero using a one-sample t-test at the 1% significance level. This analysis is repeated after progressively discarding blocks of 30, 60, 90 and 120 lead days from each forecast, to identify the lead time of member decorrelation. We consider the ensemble to be independent if the null hypothesis is accepted in at least half of the initialization months, and if the average ρ across the 12 initialization months is smaller than |0.1|. Depending on the specific characteristics of the target region, a trade-off should be found between ensuring sufficient independence across ensemble members and maximizing the sample size of the resulting pooled ensemble.

2.3.2. Creation of surrogate series

Following Klehmet et al. (2024), we generate synthetic "surrogate" time series by combining reforecast simulations initialized in different months, where each simulation is only used once. This approach enables the construction of non-overlapping forecast series that match the length of the historical dataset. The number of initialization dates required to produce a full year depends on the effective forecast length, i.e. the forecast period minus the portion of the forecast that is discarded upon assessing ensemble independence. For example, in the case of SEAS5 seasonal forecast, if member correlation is considered sufficiently low after discarding the first 30-day block, two simulations covering the remaining six months of forecast period and initialized half a year apart can be paired to form a year-long record (e.g., the forecast initialized in January and covering the period February–July will be merged with the forecast initialized in July and covering the period August-January). Using all combinations of initialization months, this 6-month surrogate type would yield a total number of 150 surrogate series spanning the period 1999–2024 (6 merging combinations × 25 ensemble members) for a total of 3900 model years. Similarly, if ensemble independence is achieved after discarding the first 90-day block, three forecasts extending over four months can be concatenated to form 4-month surrogates, yielding 100 surrogate series (4 merging combinations × 25 members for 2600 model years). The terms "surrogate series" and EFAS reforecasts are hereafter used interchangeably to refer to the synthetic time series generated from the EFAS ensemble seasonal reforecast. We note that reforecast concatenation can be successfully performed when sampling daily extremes using the annual maxima (AM) method (see Section 2.5), as this approach does not require continuity in the underlying series. In contrast, the peak-over-threshold (POT) method requires exceedances above a set threshold to be sampled from a continuous or regularly spaced series to ensure statistical independence (Coles, 2001).

2.3.3. Validation and bias correction

Statistical validation of model simulations is crucial for assessing whether EPSs are sufficiently realistic in their representation of the data extremes. Simulations of river discharge can be biased by uncertainties in the numerical weather prediction system and hydrological model parameters. If not addressed, model error may lead to unrealistic extreme events (e.g., Kelder et al., 2022b). Here, we evaluate the statistical consistency between simulated and historical discharge using a fidelity test, as in previous studies (Thompson et al., 2017, 2019; Kelder et al., 2020, 2022a). For each surrogate river discharge time series generated in Section 2.3.2, the mean, standard deviation, skewness, and kurtosis are calculated along the time dimension. A bias correction technique is introduced in order to achieve consistency with the historical time series, by verifying that all four statistical moments of the historical data fall within the 95% confidence intervals of the surrogate distributions. The optimal choice of bias correction method should be informed by the characteristics of the surrogate distribution, which are region-dependent. However, in our approach we prioritize linear multiplicative scaling, whereby the bias adjustment factor is defined as the ratio between the mean of the historical and surrogate annual maxima along the time dimension. Linear scaling is less likely to introduce additional error if compared to nonlinear bias adjustment methods such as quantile mapping (Kelder et al., 2022b), as the higher moments of the distribution are minimally altered.

2.4. Module 2: Impact assessment

2.4.1. Extreme-value analysis

We identify extremes of river discharge in the surrogate ensemble using the block maxima approach with 1-year blocks (Coles, 2001) and apply extreme-value analysis to estimate their frequency. For every grid point i in the target region, the annual maxima of daily mean discharge between 1999–2024 are extracted from each surrogate series and pooled into a single array. This procedure yields, respectively, a set of 3900 extremes for 6-month surrogates (6 merging combinations × 25 ensemble members × 26 years), 2600 extremes for 4-month

surrogates (4 merging combinations × 25 members × 26 years) and 1950 extremes for 3-month surrogates (3 merging combinations × 25 members × 26 years). Even with the most conservative surrogate construction method, pooling of EFAS reforecasts drastically increases the sample size of data extremes relative to the historical series, which only provides 26 annual maxima for the study period.

According to extreme value theory (Fisher and Tippett, 1928), independent block maxima asymptotically follow a Generalized Extreme Value (GEV) distribution, defined as:

$$F(x;\mu,\sigma,\xi)=\begin{cases}\exp\left(-\exp\left(-\frac{x-\mu}{\sigma}\right)\right) & \text{for } \xi=0 \text{ (Gumbel type),}\\ \exp\left(-\left(1+\xi\frac{x-\mu}{\sigma}\right)^{-1/\xi}\right) & \text{for } \xi\neq 0 \text{ and } 1+\xi\frac{x-\mu}{\sigma}>0.\end{cases} \quad (1)$$

where $(-\infty < \mu < \infty)$, σ (>0) and $(-\infty < \xi < \infty)$ represent the location, scale and shape parameters of the distribution, respectively. We fit the GEV distribution to the pooled ensemble of annual maxima using maximum likelihood estimation (MLE). To reduce instability of the GEV shape parameter and avoid implausible tail behaviours, we use Bayesian inference with a uniform bounded prior for $-0.3 < \xi < 0.3$ (e.g., Martins and Stedinger, 2000; Renard and Lang, 2007). The return period $T_{(x)}$ of simulated events can then be calculated from the cumulative density function $F_{(x)}$ of the fitted GEV distribution (Coles, 2001) as:

$$T_{(x)} = 1/(1 - F_{(x)}) \quad (2)$$

Extending this analysis to every grid point i, we obtain a gridded dataset of the return period of the surrogate events, $T_{(x_i)}$. We note that modelling flood events with extreme value analysis involves a degree of uncertainty related to the stability of the GEV fit, due to high sensitivity to the few largest events in the distribution. However, return periods can be estimated fairly accurately with large data samples thanks to improved estimates of tail behaviour parameters (e.g., van der Wiel et al., 2019; Macdonald et al., 2025).

2.4.2. Hazard footprint computation

We consider the buffering effect of local flood protection measures based on the FLOod PROtection Standards database (FLOPROS; Scussolini et al. 2016). FLOPROS provides modelled estimates of the return period associated with local flood defence measures. We use the local threshold value $T_{(FLOPROS)}$ to mask out grid points where $T_{(x_i)} \leq T_{(FLOPROS)}$. Hence, only the locations with return periods that would cause damage in the target region are retained. The hazard intensity, i.e. inundation height, of each UNSEEN discharge extreme is computed using flood hazard maps from the European Commission Joint Research Center (JRC, Dottori et al. 2021). The maps are produced with the LISFLOOD-FP flood inundation model (Bates and De Roo, 2000) and provide 100m-resolution flood inundation scenarios for nine reference return periods (from 1 in 10 years to 1 in 500 years) for all European river basins with an area greater than 500 km^2. Following Riedel et al. (2024), we first regrid the return period dataset onto the high-resolution grid of the flood hazard maps using the Python xESMF module (DOI: https://doi.org/10.5281/zenodo.4294774) with bilinear remapping. Secondly, we derive a gridded dataset of hazard intensity by linearly interpolating flood inundation heights from the JRC hazard maps, using the return period dimension of the two input datasets. As in Riedel et al. (2024), we introduce a capping value for the maximum flood height, assuming that this cannot exceed the local value associated with the maximum return period of 500 years in the JRC hazard maps. We note that the computation of flood hazard footprints from GloFAS (the global counterpart of EFAS, Alfieri et al. 2013) is currently implemented in CLIMADA's GloFAS River Flood Module (Riedel et al., 2024). The module employs precomputed parameters for extreme-value analysis and return period interpolation. However, the current configuration is not optimized for use with EFAS seasonal forecast data and lacks calibration for small to medium-sized watersheds. As a result, a manual adaptation of the workflow was adopted for our analysis.

2.4.3. Impact modelling

In the impact model CLIMADA, the core components of risk modelling – hazard, exposure and impact – are implemented as object-oriented classes within the software architecture. The hazard class is organized into specialized subclasses or modules representing distinct natural hazard types. The exposure and impact classes incorporate modular elements to adapt to region-specific assets and vulnerabilities. We derive economic asset exposure data from the LitPop dataset (Eberenz et al., 2021). LitPop produces gridded asset exposure data at a resolution of 30 arcseconds for 224 countries by combining population counts from NASA SEDAC's Gridded Population of the World v4.10 (GPWv4) with nightlight intensity data from NASA's Black Marble (Román et al., 2018). The core methodology of LitPop is based on the spatial disaggregation of national totals of economic indicators in proportion to population and nightlight intensity data ($GDP \propto Lit^m * Pop^n$). LitPop is available as a built-in class in CLIMADA with user-defined attributes that determine the indicator to use as the total asset value for disaggregation. For our analysis, we consider gridded physical asset value derived from the disaggregation of national produced capital, using the most recent available year as reference. Produced capital stock (World Bank, 2019) has been extensively used as an indicator of the value of manufactured and built assets exposed to natural disasters (Eberenz et al., 2021). The impact calculation functions in CLIMADA first align the hazard intensity data with the corresponding exposure coordinates. Then, flood footprints are converted to a damage factor derived from continental depth-damage functions provided by the JRC (Huizinga et al., 2017). The damage functions are available at the continental scale, but they serve as guidelines for damage assessments at the national level for countries where stage-damage curves are not available (e.g., Carisi et al., 2018). We obtain the estimated economic damage (*EED*) of each UNSEEN event as the total direct economic loss in the target basin, allowing a comparative ranking of events by impact. The EED-ranked UNSEEN events are labelled with a unique identifier that combines their surrogate initialization month and ensemble member. For instance, the event occurring on October 5, 2007 simulated by the ensemble member 03 of the surrogate series starting in July, will have event ID S:Jul-m3-2007-10-05.

2.5. Module 3: Creation of the UNSEEN event catalogue

We narrow down the set of UNSEEN flood events to those with the greatest direct economic impact by selecting the 100 events with the highest EED. To assess the synoptic conditions associated with high impact events, we examine the mean sea level pressure (MSLP) and geopotential height at 500hPa (Z500) from SEAS5 simulations. Because SEAS5 is used to force EFAS reforecasts, the two products align in terms of ensemble members, initialization dates, and temporal coverage; this enables the construction of SEAS5 surrogate series following the same procedure adopted for EFAS (Section 2.3.2). Using the event identifiers, we match the 100 high impact UNSEEN events with the corresponding Z500 and MSLP fields from the daily SEAS5 surrogate series. However, because daily discharge in EFAS is defined as the discharge accumulated in the last 24 h, we shift their timestamps backwards by one day when identifying the matching MSLP/Z500 fields. The final set of events represents the UNSEEN event catalogue for the target region, storing information on (i) river discharge at target locations along the river, or mean/maximum discharge across the basin, (ii) the flood footprint or hazard intensity, (iii) the estimated economic damage in the river basin, and (iv) the MSLP and Z500 fields on the day of each event. In Section 3, we show how the UNSEEN event catalogue can be further analysed to anticipate historical flood events at the regional level.

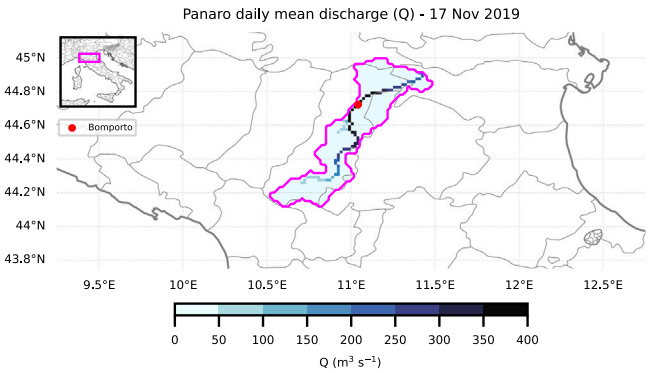

Fig. 2. The Panaro watershed in Emilia-Romagna, Italy. Contours indicate EFAS river discharge on the day of maximum discharge recorded between 1999–2024 (17 November 2019). The magenta basin outline is derived from the HydroBASINS dataset; the red dot marks the location of Bomporto hydrometric station.

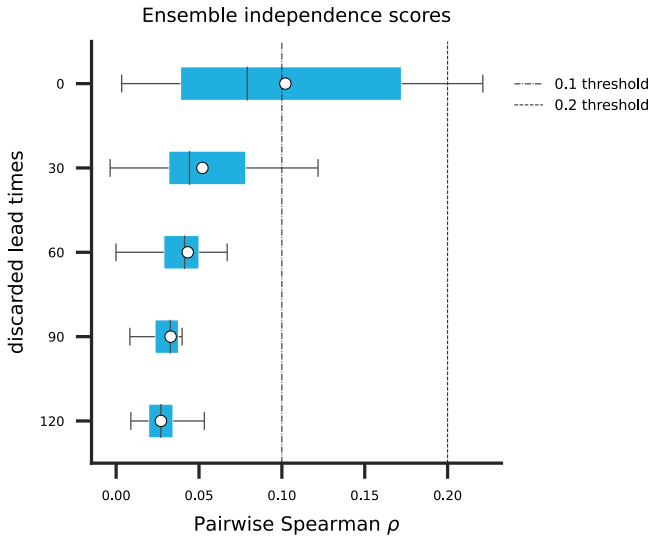

Fig. 3. Ensemble independence scores of EFAS seasonal reforecasts as a function of number of discarded lead times (i.e., number of days since forecast initialization) for the closest grid point to the Bomporto station. Independence scores are calculated as the average pairwise Spearman correlation among the 25 ensemble members for each initialization month. Vertical dashed lines highlight correlation levels of 0.1 and 0.2. The mean and median ensemble correlation across the 12 initialization months are marked with a white dot and a black line, respectively.

3. Case study

The northern Italian region of Emilia-Romagna, located in the eastern sector of the Po Valley, is frequently exposed to river flooding and storm surge events. River flooding in Emilia-Romagna is typically the result of isolated storms or mesoscale organized convection (Shah et al., 2023). The region experienced exceptional flooding in May 2023 as a result of short but heavy rainfall events linked to three distinct Mediterranean cyclones (Barnes et al., 2023; Cremonini et al., 2024; Dorrington et al., 2024). The combination of floods and landslides caused the displacement of thousands of residents, casualties and severe economic damage over €9 billion. In some locations, the severity of these events was estimated to correspond to return periods exceeding 500 years, underscoring the urgent need to reassess existing flood defence strategies (Brath et al., 2023).

We illustrate the case study of the Panaro river (Fig. 2), a medium-sized river (drainage basin ~ 1775 km^2) that serves as the final right-hand tributary of the Po river. Despite its modest scale, the Panaro is prone to severe flooding due to the combined effects of high-flow events and riverbank instability (e.g., Dazzi et al., 2022). Record-breaking floods occurred in November 2019 as part of a broader pattern of extreme weather events affecting the region (ARPAE Emilia-Romagna, 2019) and in December 2020 as a result of intense rainfall combined with snow melt (ARPAE Emilia-Romagna, 2021). A more recent episode of flooding occurred in 2024 as a result of the Mediterranean cyclone "Boris" (September 16–19, 2024), which stalled over northern Italy due to a blocking anticyclone over Northern Europe, leading to intense and prolonged rainfall across Emilia-Romagna (Foraci et al., 2024). Recent risk assessments have attributed a "Medium-High to High" risk score to a large number of municipalities surrounding the Panaro river, due to elevated exposure and vulnerability levels. The basin area has also been selected as one of the Open Air Laboratories (OALs) where flood risk could be successfully mitigated with nature-based solutions (Shah et al., 2023) as part of the OPERANDUM H2020 Project. Our focus on a medium-sized basin is not only motivated by the scientific and societal relevance of recent extreme events, but also by the fact that the UNSEEN methodology and most impact assessments studies have so far concentrated on larger national-scale systems, whereas medium-sized basins are typically studied with traditional hydrological models.

3.1. Reforecast validation

Following the methodology described in Section 2.3, we first validate EFAS reforecasts by assessing whether the 25-member ensemble is sufficiently independent and statistically consistent with historical data. Fig. 3 presents ensemble independence scores as a function of discarded lead times (i.e., the number of days after the forecast initialization date), where box-and-whisker plots indicate the distribution of the average pairwise Spearman correlation coefficients across the 12 initialization months. Independence scores are calculated for river discharge at a representative location corresponding to the nearest grid point to the hydrometric station at Bomporto, located mid-river course (44.72°N, 11.04°E) and used hereafter as reference grid point for the basin. When discarding more than 30 lead days, independence scores are consistently below the correlation threshold of 0.2, with interquartile ranges less than 0.1, indicating a satisfactory degree of ensemble independence. Given that blocks of 3, 4, or 6 months can be concatenated to form a full year from the original 215-day (~7-month) forecasts, we identify 90 days as the optimal number of lead times to discard from the original forecasts. The pairwise correlations of individual initialization months with this configuration are shown in Figure S2 in the Supplementary Material. Our 90-day cutoff is broadly consistent with Klehmet et al. (2024), who assume ensemble independence after the first 4 months of forecast in a pan-European study. After removing the initial 90-day period from each forecast, the remaining 4-month forecast blocks from three initialization dates are concatenated to form a full year, i.e. a 4-month surrogate series. Using each initialization date once, we generate four surrogate ensembles with 25 members each, yielding a total of 100 surrogate time series covering the period 1999–2024.

The results of the fidelity test are shown in Fig. 4, where the higher statistical moments of annual maximum discharge in the surrogate and historical series are compared, both with and without bias correction. In the unadjusted distribution, model bias results in underestimation of the mean and standard deviation relative to the historical series (227.7 and 93.9 m^3 s^{-1}, respectively — vertical dashed lines in Fig. 4a-b), while skewness and kurtosis are consistent (Fig. 4c-d). The biased low river discharge in the surrogate data is compatible with SEAS5's limited rainfall predictability over land, in part associated with its relatively coarse (~36 km) resolution (Johnson et al., 2019). However, bias correction with linear multiplicative scaling is sufficient

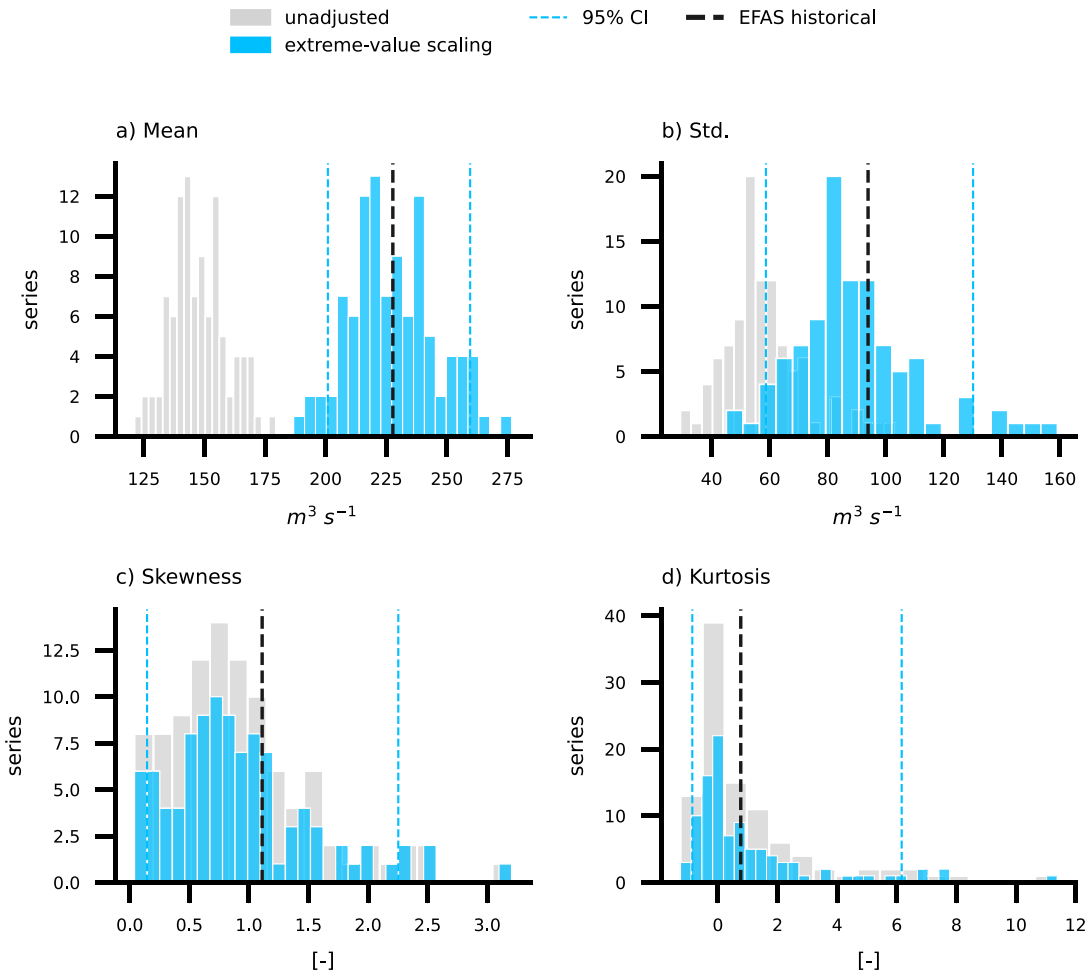

Fig. 4. Fidelity test assessing the consistency between EFAS reforecast and historical discharge for the Panaro river at the grid point closest to Bomporto station. The mean, standard deviation, skewness and kurtosis of each EFAS surrogate series of annual maxima is computed along the time dimension and compared with the historical time series (black dashed line). Grey distributions indicate the unadjusted surrogate data; blue distributions show bias corrected surrogates via extreme-value scaling. Thin blue dashed lines mark the 95% confidence intervals of the surrogate distributions.

to adjust the mean and variance of the reforecast ensemble when applied directly to the annual maxima. With this method, the surrogate distribution is scaled by a factor defined as the ratio between the mean historical and reforecast annual maxima, directly targeting the relative quantile. The statistical moments of historical data fall within the 95% confidence intervals of the surrogate distribution, indicating good agreement between the datasets. Alternative approaches for bias correction have been explored: linear multiplicative scaling based on all daily data fails to adjust the mean and variance relative to the historical data (Figure S3a), while quantile mapping exhibits tendencies towards overfitting and artificial distortion of the tail of the distribution (not shown); therefore, its application is excluded. As in Fig. 3, the results of the fidelity test in Fig. 4 reflect a representative grid point nearest Bomporto station, but we find consistent results when applying the test to different locations along the river course (not shown).

3.2. Identifying unrealized extremes

Fig. 5a shows the distributions of unadjusted and bias corrected annual maxima of daily discharge. When pooling together all annual maxima from the surrogate series, we obtain a sample of 2600 extremes (100 series × 26 years), exactly 100 times larger than the historical extreme sample. The extreme-value fits and empirical return periods of the historical and simulated annual maxima, estimated with the Weibull plotting position formula, are presented in Fig. 5b. Due to their small number, historical annual maxima are modelled with a Gumbel fit (that is, a GEV with $\xi = 0$), with 95% confidence intervals extracted via bootstrap resampling (grey shading in Fig. 5b). The large uncertainty bands of the Gumbel fit and the relatively poor alignment between theoretical and empirical return levels highlight that inferences based on historical extremes are imprecise given the scarcity of events. Surrogate extremes, on the other hand, are fitted with a GEV distribution since the shape parameter is generally estimated with better accuracy from a large ensemble size. Applying the GEV fit to the gridded discharge data yields values of ξ between −0.2 and 0.2 and centred around 0 (−0.026), suggesting that discharge extremes in the Panaro river follow a light-tailed GEV distribution. The bias corrected time series of UNSEEN annual maxima is displayed in Fig. 6 alongside historical annual maxima. The record-breaking historical event of November 2019, with a peak discharge of 488.3 $m^3\ s^{-1}$ at Bomporto, is exceeded by 40 UNSEEN events from the bias-corrected distribution (Fig. 6) and 3 UNSEEN events from the unadjusted distribution (not shown).

3.3. Synoptic event catalogue

Following the procedure described in Section 2.4–Section 2.5, we generate a catalogue of the 100 flood events with the highest EED as computed with CLIMADA. Flood defence measures for the Panaro river are designed to provide protection against events with a return period of 50 years (Scussolini et al., 2016). Therefore, the calculated EED

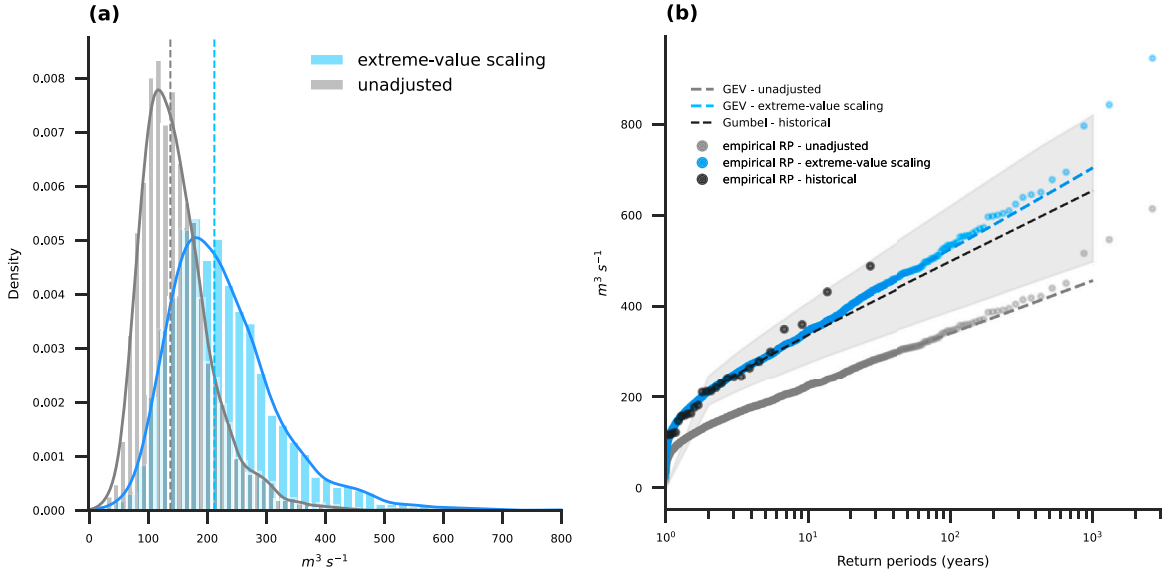

Fig. 5. Distributions (**a**) and extreme-value fits (**b**) of annual maxima of daily discharge sampled from surrogate series (no bias correction — grey; extreme-value scaling — blue). The black dashed line in panel (**b**) shows a Gumbel fit applied to historical annual maxima, with light grey shading indicating 95% confidence intervals; all other fits are estimated with a Generalized Extreme Value (GEV) distribution. Dots mark empirical return periods estimated with the Weibull plotting position formula. Note the log-scale of the *x*-axis in panel (**b**).

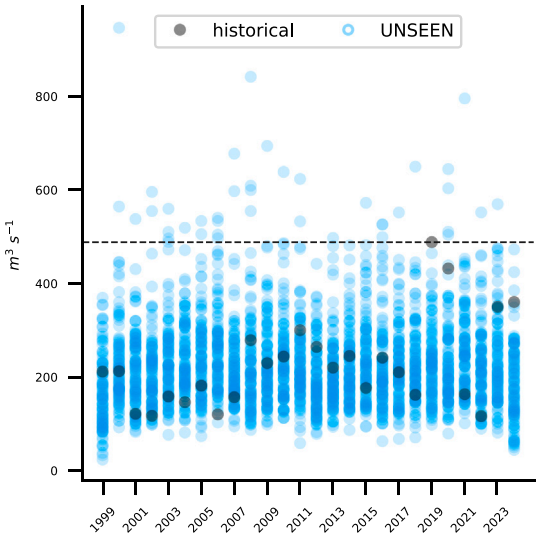

Fig. 6. Historical (black) and bias-corrected UNSEEN (blue) annual maximum daily mean discharge at Bomporto. The horizontal dashed line marks the historical record-breaking peak in November 2019 (488.3 $m^3\ s^{-1}$).

of UNSEEN events in this region reflects the total damage associated with hazard footprints that exceed this level of protection (Scussolini et al., 2016). The highest EED (~591.0 million USD) is attributed to the event on 06-10-2007 simulated by member 3 of the surrogate series starting in July (event ID: S:Jul-m3-2007-10-06). Fig. 7a shows the MSLP and Z500 fields associated with the record-breaking event of 17 November 2019 (488 $m^3\ s^{-1}$ at Bomporto) and the eight top-ranking UNSEEN events by EED (Fig. 7b-i). Note that Z500 and MSLP fields for the historical event in Fig. 7a are taken from the ERA5 reanalysis. The UNSEEN events shown in Fig. 7b-i generally exhibit levels of discharge that exceed the November 2019 event, with peaks at gridpoint equivalent to Bomporto ranging from 486 $m^3\ s^{-1}$ (Fig. 7(e) to 676 $m^3\ s^{-1}$ (Fig. 7(b). The three UNSEEN events with the highest discharge at Bomporto (945, 840 and 794 $m^3\ s^{-1}$, respectively; Fig. 6) were not assigned a hazard footprint or damage label as their return periods exceed the imposed capping value of T = 500 years used in the hazard footprint computation (Section 2.4.2), consistent with the upper bound of flood hazard maps, Dottori et al., 2021). For all other UNSEEN events, a clear coupling emerges between elevated discharge and high EED (Figure S4).

Recurrent synoptic patterns in the 100-event catalogue are identified with multivariate k-means clustering (Hartigan and Wong, 1979). Daily Z500 and MSLP fields are de-seasonalized and detrended by removing a daily climatological mean and the 1999–2024 linear trend. The anomaly fields of each event are then concatenated and standardized into a combined Z500/MSLP feature input. The k-means analysis is performed in the region bounded by latitudes between 30°N–70°N and longitudes between 20°W–20°E to focus on the large-scale circulation. We identify the optimal number of clusters centroids as k = 2 based on the Silhouette, Davidson-Bouldin, and Calinski-Harabasz evaluation criteria for k-means classification (Silhouette = 0.183, CH = 25.7, DB = 1.879; Figure S5). The dominant patterns of atmospheric circulation anomalies associated with high impact floods in the Panaro basin are shown in Fig. 8a-b, with the events in Fig. 8c-d representing particularly extreme examples of each configuration in terms of EED. Consistent with Fig. 7, the clustered patterns in Fig. 8 suggest that a deep cyclone over central-western Italy or a deep trough over western Europe with an eastern flank over Italy are favourable synoptic conditions for flooding in Emilia-Romagna. These circulation types are broadly consistent with two of the four weather patterns causing precipitation extremes in the Emilia Romagna region (Iacomino et al., 2025). We find no substantial differences in applying the clustering analysis to catalogues with fewer or more events. Consistent synoptic patterns to those shown in Fig. 8a-b emerge after clustering the top 50 or top 200 highest-ranking events by EED (not shown).

We finally demonstrate that the UNSEEN event catalogue can be used to anticipate noteworthy historical extremes. We identify circulation analogues for the November 2019 and December 2020 flood events – the largest and second largest historical discharge events at Bomporto, respectively – among the 100 high-impact events included in the UNSEEN catalogue. We select the most suitable analogue by maximizing the pointwise Spearman correlation coefficient (ρ) between the Z500 and MSLP raw fields of each UNSEEN event and the corresponding field

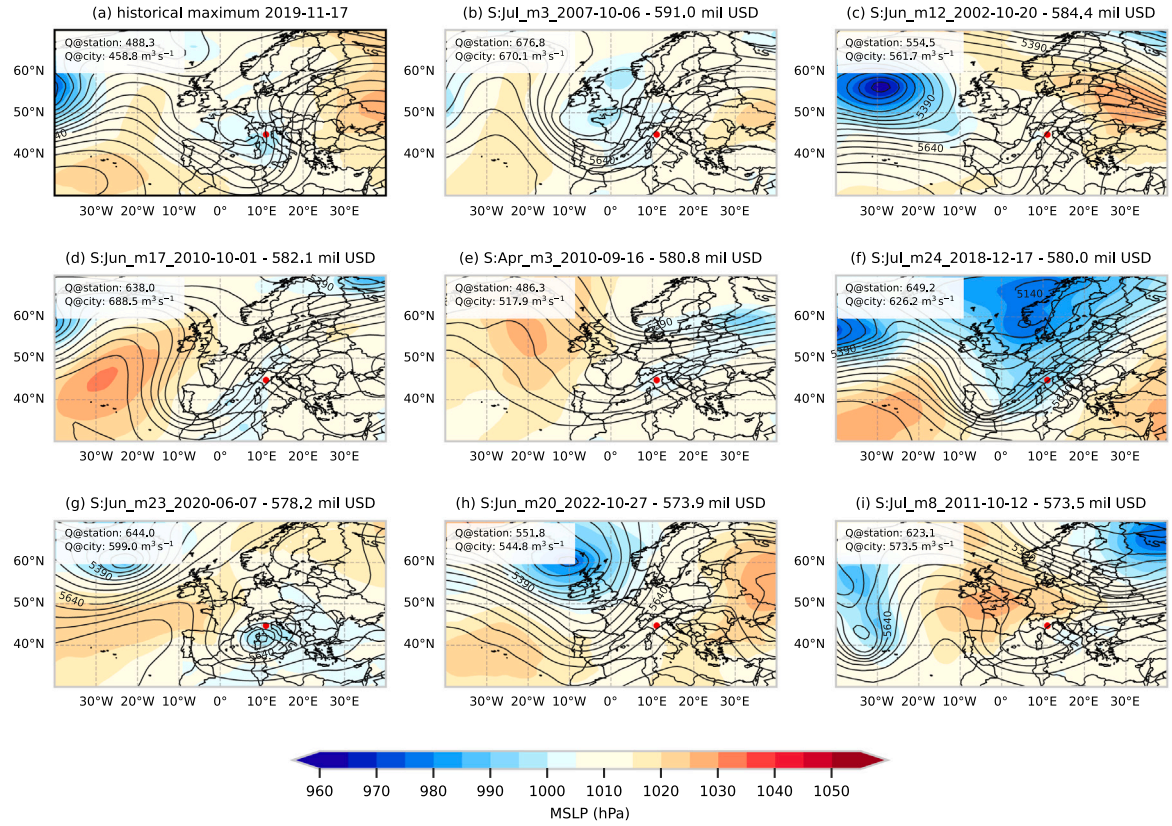

Fig. 7. Mean sea level pressure (colour shading) and geopotential height at 500hPa (black contours) associated with the record-breaking historical event by river discharge at Bomporto (**a**) and the eight UNSEEN events with the largest estimated economic damage (EED, expressed in million USD in **b-i**). MSLP and Z500 fields are taken from ERA5 in (**a**) and SEAS5 in (**b-i**). Annotations show bias corrected EFAS discharge at the grid point corresponding to Bomporto station (Q@station) and in proximity of the largest city, Modena (Q@city). UNSEEN events in (**b-i**) are plotted in descending order of EED. The red dot in each panel marks the location of the target region.

in the historical event, after flattening and concatenating the two fields. The 2019 and 2020 historical extremes and their closest analogues are presented in Fig. 9. In both cases, the atmospheric circulation of historical floods can be paired to a high impact UNSEEN counterpart simulated in the autumn of previous years (October 2015, $\rho = 0.834$ and October 2007, $\rho = 0.825$, respectively). Remarkably, the most suitable analogue for the December 2020 historical flood corresponds to the UNSEEN event with the highest impact in the entire 2600-event surrogate ensemble (ID: S:Jul-m3-2007-10-06), with an of 591.0 million USD and a simulated discharge of 676.8 $m^3 s^{-1}$ at Bomporto.

4. Concluding remarks

We have presented a customizable framework to generate a catalogue of unprecedented high impact flood events in European river catchments using the EFAS and SEAS5 ensemble prediction systems. The framework builds on existing methodologies for ensemble reforecast pooling and validation (e.g., Thompson et al., 2017; Kelder et al., 2022a) as well as hazard computation for impact modelling (Riedel et al., 2024). Motivated by the notion that rare meteorological events do not necessarily cause high socio-economic impact (e.g., van der Wiel et al., 2019) and vice versa, we leveraged the probabilistic risk model CLIMADA to identify flood events with high impact potential. The final event set provides a physically-based foundation for detecting severe events that may occur in the near-term but have few, if any, historical precedents.

The case study of the Panaro river in Emilia-Romagna demonstrates that the framework can be successfully applied to medium-sized river basins, provided that the validation tests yield successful outcomes (Section 2.3). In our case study, we found that the 25-member ensemble of EFAS seasonal reforecast is sufficiently independent after 90 days from the initialization date. This enabled the construction of 100 independent surrogate time series of river discharge for the 26-year period between 1999–2024, equivalent to 2600 synthetic annual maxima. We have shown that the statistical characteristics of the surrogate series align well with the EFAS historical data, except for a tendency of the modelled data to underestimate the mean discharge of extreme events, which can be corrected with linear scaling. The pooled distribution of synthetic annual maxima is effectively captured by the GEV fit, as indicated by the close agreement between theoretical and empirical return levels (Fig. 5). Furthermore, despite the relatively small region size, the hazard footprint of UNSEEN events could be linearly interpolated from flood hazard maps (Dottori et al., 2021), owing to the fine spatial resolution of this product. Crucially, the Panaro case study underscores the added value of using a catalogue of UNSEEN high impact events to anticipate record-breaking historical floods. Analogue analysis revealed that the synoptic circulation pattern associated with the historical event of December 2020 closely resembles that of the UNSEEN event simulated in October 2007, with a 38.7% increase in river discharge at the Bomporto river gauge and an estimated damage of 591.0 million USD, the highest in the event ensemble. We note that our definition of an event catalogue differs from that used in previous work. For example, Paprotny et al. (2024a) developed a comprehensive modelling chain to support a factual reconstruction of past coastal and riverine flood events that caused significant socio-economic losses, using the ERA5 and ERA5-Land reanalyzes along with the HANZE

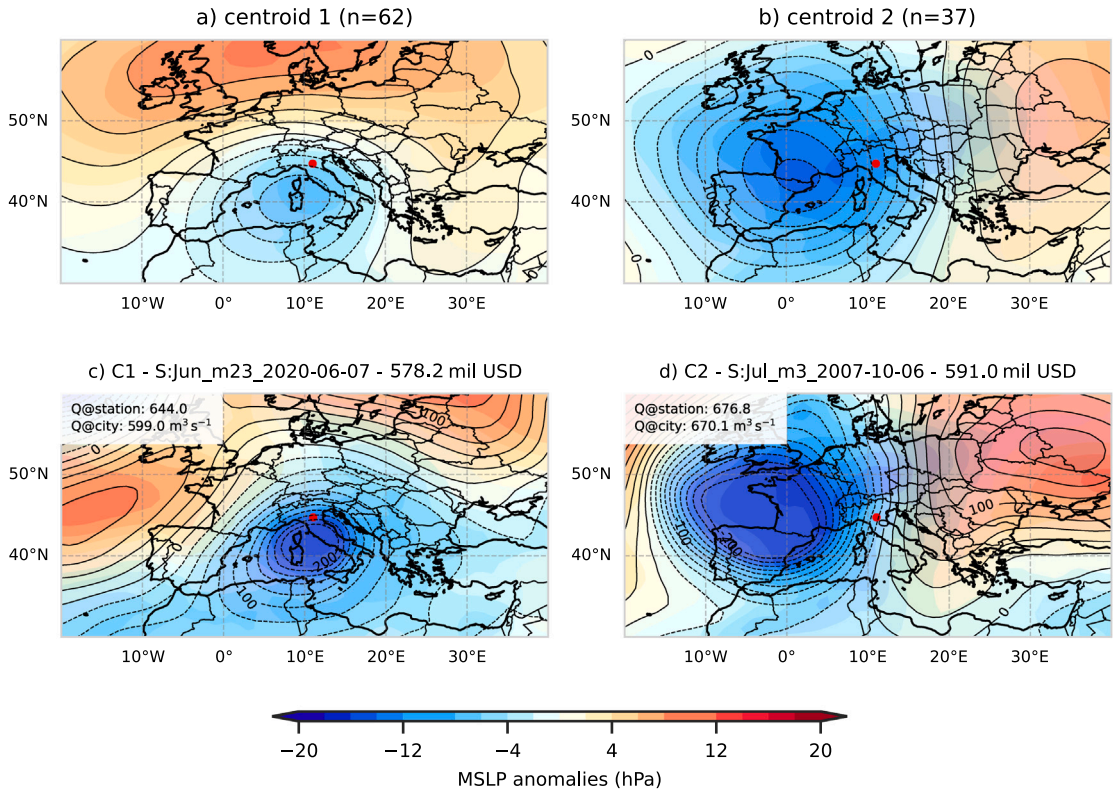

Fig. 8. (**a-b**) K-means clusters of mean sea level pressure anomalies (colour shading) and 500hPa geopotential height anomalies (black contours - dashes indicate negative values) associated with the top 100 UNSEEN events by EED (n_{tot} = 100). (**c-d**) Highest-impact event in each cluster. MSLP and Z500 daily fields are de-seasonalized and detrended by removing a daily climatological mean and the 1999–2024 linear trend. As in Fig. 7, annotations show bias corrected discharge values at Bomporto station (Q@station) and nearest the city of Modena (Q@city).

impact dataset (Paprotny et al., 2024b). In contrast, our event set represents a collection of plausible alternative realizations of the recent historical period and their relative estimated impacts. In this sense, the catalogue can be used to inform decisions under uncertainty and help local operational services evaluate potential response strategies.

The methodology presents some challenges and limitations that require careful evaluation of the input data characteristics for the specific region under study. First, the simulated river discharge extremes are sensitive to errors and approximations propagating from the physical model simulations. While systematic biases can be corrected using historical or observed data as a benchmark, statistical adjustments to the modelled distribution may introduce spurious or unrealistic extremes. Additionally, certain properties of the pooled event distribution can affect the stability of the extreme value fit, potentially undermining the robustness of the return period estimation. A tailored approach may be required to suit the size and specific characteristics of the data distribution. For example, different approaches to sampling extremes, such as increasing the length of the sampling blocks to 5 or 10 years, may be necessary to achieve asymptotic convergence of the block maxima distribution to the GEV limit (Ben Alaya et al., 2020). Further uncertainties stem from the flood height interpolation described in Section 2.4.2. Although JRC maps represent the most comprehensive flood hazard dataset available, validation tests (Dottori et al., 2021) indicate low model skill for high- to medium-probability events, resulting in significant hazard overestimation. The interpolation accuracy is also affected by the coarse resolution of the return periods, which provides only nine steps. We also note that nominal (i.e., policy-defined) structural defence standards included in the FLOPROS dataset have been shown to be overestimated (Paprotny et al., 2025). However, this bias is unlikely to affect our results, given that the framework is designed for the largest events, i.e., with much higher return periods. Finally, the limited availability of empirical damage data – currently relying on spatial disaggregation techniques and continental-scale damage functions – requires caution when interpreting estimated economic damage for UNSEEN events. The assessment of damage is further complicated by the spatio-temporal misalignment between the meteorological event and the socio-economic impact, a known challenge in extreme event attribution research (Philip et al., 2020; Perkins-Kirkpatrick et al., 2022; Van Oldenborgh et al., 2021). Despite these uncertainties, the extensive volume of data incorporated in the modelling chain and the physical robustness of ensemble simulations represent important advantages over conventional methods that rely solely on historical data. With continued advances in computational power and capacity, climate services such as EPS provide an invaluable tool to improve the prediction of extreme events and promote risk preparedness. Although the framework we have described is not directly applicable to other hazard types, it can be easily adapted to accommodate weather-related extremes for which ensemble seasonal reforecasts are available, especially tropical cyclones and wildfires as these are already included in CLIMADA.

An in-depth assessment of the physical drivers of high-impact flood events was beyond the scope of our analysis. However, the severity of flood damage depends on many factors, such as the persistence of cyclones and cutoffs (e.g., Yamamoto et al., 2024; Thompson et al., 2025), soil saturation (e.g., Tramblay et al., 2023) and flow velocity (e.g., Amadio et al., 2019). These factors are crucial in distinguishing disastrous events from other events with similarly favourable meteorological drivers. Future work could address this aspect by introducing additional criteria for UNSEEN event selection, to analyse how impacts may change in response to specific preconditioning processes. Recent literature has highlighted the added value of using causal networks (Shepherd, 2019; Rodrigues and Shepherd, 2022) to explore

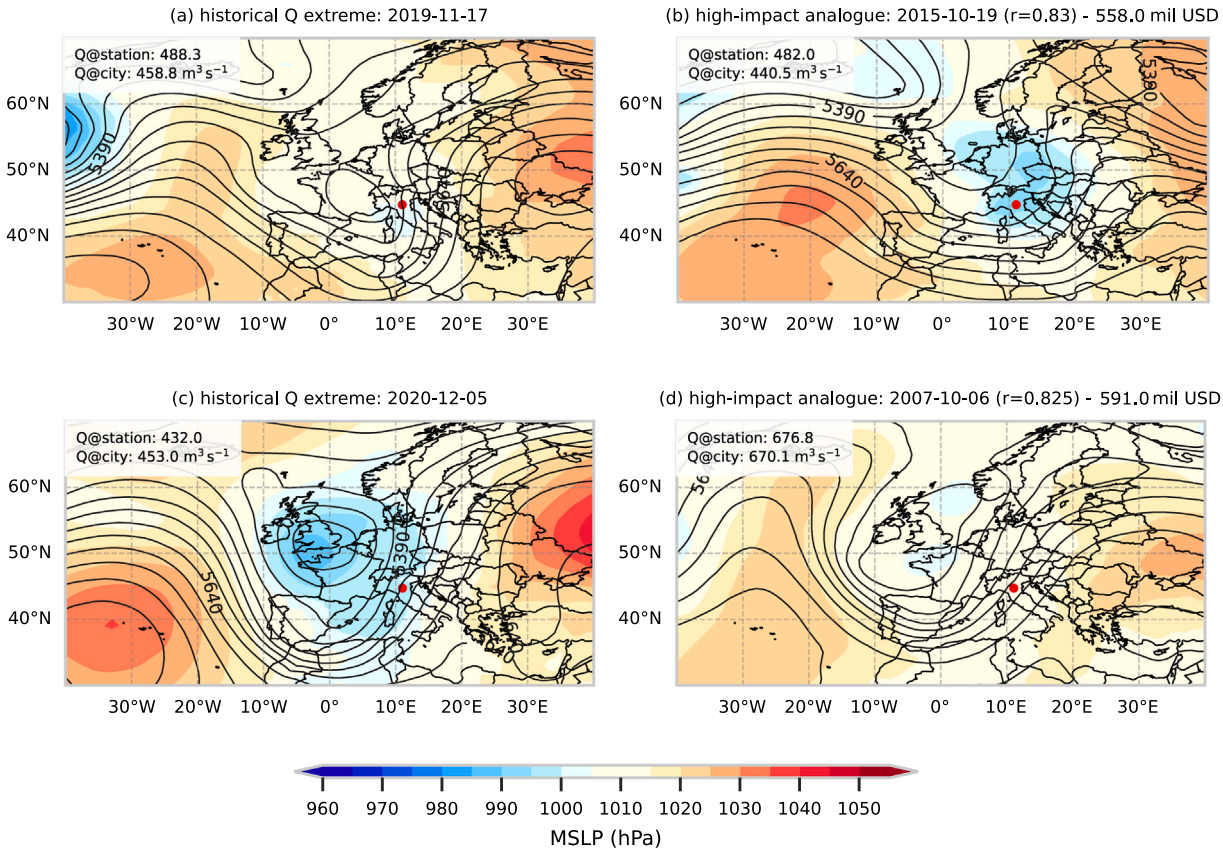

Fig. 9. (a-b) Z500 (black contours) and MSLP (colour shading) associated with the record-breaking historical event by discharge at Bomporto (November 2019 - **a**) and its closest analogue in the UNSEEN catalogue (**b**). **(c-d)** as in **(a-b)**, but showing the second largest historical event (December 2020 - **c**) and its closest UNSEEN analogue (**d**).

the links between drivers, impacts and feedbacks, where causes and counterfactuals are examined through conditional hypotheses (Pearl, 2009). Reducing the uncertainty associated with the cause–effect relationships of high-impact events is integral for promoting a transition from reactive adaptation (i.e., in response to disasters) to incremental, long-term adaptation (Kelder et al., 2025). By placing emphasis on the plausibility range of events, record-breaking extremes in the future will be unprecedented, but not unexplored.

CRediT authorship contribution statement

Elena Bianco: Writing – original draft, Visualization, Software, Investigation, Formal analysis, Data curation. **Paolo Davini:** Writing – review & editing, Software, Data curation, Conceptualization. **Giuseppe Zappa:** Writing – review & editing, Data curation, Conceptualization. **Agostino Manzato:** Writing – review & editing, Investigation, Data curation. **Antonio Giordani:** Writing – review & editing, Investigation. **Paolo Ruggieri:** Supervision, Resources, Project administration, Investigation, Conceptualization.

Funding

This work was supported by NextGenerationEU as part of the PRIN PNRR 2022 project TRANSLATE - climaTe Risk informAtion from eNSembLe weAther and climaTe prEdictions.

Declaration of competing interest

The authors declare that they have no known competing financial interests or personal relationships that could have appeared to influence the work reported in this paper.

Acknowledgements

We thankfully acknowledge Prof. Silvana Di Sabatino for providing valuable insights during the conceptualization and discussion phases.

Appendix A. Supplementary data

Supplementary material related to this article can be found online at https://doi.org/10.1016/j.cliser.2026.100636.

Data availability

The published catalogue of high-impact UNSEEN events for the Panaro river can be found on Zenodo at https://zenodo.org/records/18260378 (DOI: 10.5281/zenodo.18260378). River discharge data from the European Flood Awareness System can be accessed from the Copernicus Emergency Management Service (CEMS) Early Warning Data Store at https://ewds.climate.copernicus.eu/datasets/efas-historical?tab=download. Ensemble seasonal reforecasts are also available from CEMS at https://ewds.climate.copernicus.eu/datasets/efas-reforecast?tab=download. Seasonal reforecasts of meteorological variables from ECMWF SEAS5 can be downloaded from the Copernicus Climate Data Store (CDS) at https://cds.climate.copernicus.eu/datasets/seasonal-original-single-levels?tab=downloadfor single-level variables and at https://cds.climate.copernicus.eu/datasets/seasonal-original-pressure-levels?tab=download for pressure-level variables. The ECMWF ERA5 reanalysis is available at https://www.ecmwf.int/en/forecasts/dataset/ecmwf-reanalysis-v5. Users can find information on how to install and run CLIMADA at https://climada-python.readthedocs.io/en/stable/.

HydroBASINS vectorized polygon layers providing basin boundaries can be found at https://www.hydrosheds.org/products/hydrobasins.

References

Alfieri, L., Burek, P., Dutra, E., Krzeminski, B., Muraro, D., Thielen, J., Pappenberger, F., 2013. Glofas – global ensemble streamflow forecasting and flood early warning. Hydrol. Earth Syst. Sci. 17 (3), 1161–1175. http://dx.doi.org/10.5194/hess-17-1161-2013.

Amadio, M., Scorzini, A.R., Carisi, F., Essenfelder, A.H., Domeneghetti, A., Mysiak, J., Castellarin, A., 2019. Testing empirical and synthetic flood damage models: the case of Italy. Nat. Hazards Earth Syst. Sci. 19 (3), 661–678.

Aon Impact Forecasting, 2024. Floods in eastern and southern Spain of october 2024 (event recap as of october 31). https://fundacionaon.es/wp-content/uploads/2024/11/Spain-Flooding-Impactforecasting.pdf. (Accessed 20 August 2025).

ARPAE Emilia-Romagna, 2019. Report dell'evento meteorologico dal 15 al 19 novembre 2019. (Accessed 01 July 2025).

ARPAE Emilia-Romagna, 2021. Evento meteorologico e idrologico 04–08 dicembre 2020. Tech. rep., Regione Emilia-Romagna, Allerta Meteo, Bologna, Italy, URL https://allertameteo.regione.emilia-romagna.it/documents/20181/437770/Evento+04-08+dicembre+2020.pdf. (Accessed: 01 July 2025).

Aznar-Siguan, G., Bresch, D.N., 2019. CLIMADA v1: a global weather and climate risk assessment platform. Geosci. Model. Dev. 12 (7), 3085–3097.

Barnes, C., Faranda, D., Coppola, E., Grazzini, F., Zachariah, M., Lu, C., Kimutai, J., Pinto, I., Pereira, C., Sengupta, S., et al., 2023. Limited net role for climate change in heavy spring rainfall in emilia-romagna. World Weather. Attrib. Rep. 10, 104550.

Bates, P.D., De Roo, A., 2000. A simple raster-based model for flood inundation simulation. J. Hydrol. 236 (1–2), 54–77.

Ben Alaya, M.A., Zwiers, F., Zhang, X., 2020. An evaluation of block-maximum-based estimation of very long return period precipitation extremes with a large ensemble climate simulation. J. Clim. 33 (16), 6957–6970.

Blöschl, G., Hall, J., Viglione, A., Perdigão, R.A.P., Parajka, J., Merz, B., Lun, D., et al., 2019. Changing climate both increases and decreases European river floods. Nature 573 (7772), 108–111. http://dx.doi.org/10.1038/s41586-019-1495-6.

Brath, A., Casagli, N., Marani, M., Mercogliano, P., Motta, R., 2023. Rapporto della Commissione tecnico-scientifica sugli eventi meteorologici estremi del maggio 2023. Tech. rep., Regione Emilia-Romagna, Bologna, Coordinated by A. Brath. (Accessed 27 August 2025).

Van den Brink, H., Können, G., Opsteegh, J., van Oldenborgh, G.J., Burgers, G., 2004. Improving 104-year surge level estimates using data of the ecmwf seasonal prediction system. Geophys. Res. Lett. 31 (17).

Brunner, M.I., Slater, L.J., 2022. Extreme floods in europe: going beyond observations using reforecast ensemble pooling. Hydrol. Earth Syst. Sci. 26 (2), 469–482.

Carisi, F., Schröter, K., Domeneghetti, A., Kreibich, H., Castellarin, A., 2018. Development and assessment of uni-and multivariable flood loss models for emilia-romagna (Italy). Nat. Hazards Earth Syst. Sci. 18 (7), 2057–2079.

Chan, W.C., Arnell, N.W., Darch, G., Facer-Childs, K., Shepherd, T.G., Tanguy, M., 2024. Added value of seasonal hindcasts to create UK hydrological drought storylines. Nat. Hazards Earth Syst. Sci. 24 (3), 1065–1078.

Chan, W.C., Shepherd, T.G., Facer-Childs, K., Darch, G., Arnell, N.W., 2022. Storylines of UK drought based on the 2010–2012 event. Hydrol. Earth Syst. Sci. 26 (7), 1755–1777.

Ciullo, A., Martius, O., Strobl, E., Bresch, D.N., 2021. A framework for building climate storylines based on downward counterfactuals: The case of the European union solidarity fund. Clim. Risk Manag. 33, 100349.

Coles, S.G., 2001. An Introduction to Statistical Modeling of Extreme Values. Springer Series in Statistics, http://dx.doi.org/10.1007/978-1-4471-3675-0.

Cremonini, L., Randi, P., Fazzini, M., Nardino, M., Rossi, F., Georgiadis, T., 2024. Causes and impacts of flood events in emilia-romagna (Italy) in may 2023. Land 13 (11), 1800.

Curipoma-Viteria, A., Cerpa, G.O., Blade, E., 2023. Counterfactual analysis applied to flood risk in relation to climate change. In: SimHydro. Springer, pp. 429–447.

Dazzi, S., Vacondio, R., Mignosa, P., Aureli, F., 2022. Assessment of pre-simulated scenarios as a non-structural measure for flood management in case of levee-breach inundations. Int. J. Disaster Risk Reduct. 74, 102926.

Donat, M.G., Lowry, A.L., Alexander, L.V., O'Gorman, P.A., Maher, N., 2016. More extreme precipitation in the world's dry and wet regions. Nat. Clim. Chang. 6 (5), 508–513.

Dorrington, J., Wenta, M., Grazzini, F., Magnusson, L., Vitart, F., Grams, C.M., 2024. Precursors and pathways: Dynamically informed extreme event forecasting demonstrated on the historic emilia-romagna 2023 flood. Nat. Hazards Earth Syst. Sci. 24 (9), 2995–3012.

Dottori, F., Alfieri, L., Bianchi, A., Skoien, J., Salamon, P., 2021. A new dataset of river flood hazard maps for europe and the mediterranean basin region. Earth Syst. Sci. Data Discuss. 2021, 1–35.

Eberenz, S., Lüthi, S., Bresch, D.N., 2021. Regional tropical cyclone impact functions for globally consistent risk assessments. Nat. Hazards Earth Syst. Sci. 21, 393–414. http://dx.doi.org/10.5194/nhess-21-393-2021.

Fischer, E.M., Beyerle, U., Bloin-Wibe, L., Gessner, C., Humphrey, V., Lehner, F., Pendergrass, A.G., Sippel, S., Zeder, J., Knutti, R., 2023. Storylines for unprecedented heatwaves based on ensemble boosting. Nat. Commun. 14 (1), 4643. http://dx.doi.org/10.1038/s41467-023-40112-4.

Fisher, R.A., Tippett, L.H.C., 1928. Limiting forms of the frequency distribution of the largest or smallest member of a sample. In: Mathematical Proceedings of the Cambridge Philosophical Society, vol. 24, (2), Cambridge University Press, pp. 180–190.

Foraci, R., Grazzini, F., Aguzzi, M., Fornasiero, A., Unguendoli, S., Zenoni, E., Pavan, V., Antolini, G., Pizziolo, M., Perini, L., 2024. Rapporto degli eventi meteorologici di piena e di frana del 17–19 settembre 2024. Tech. rep., Arpae Emilia-Romagna, Struttura Idro-Meteo-Clima, Bologna, Published 02 December 2024.

Furrer, E.M., Katz, R.W., 2008. Improving the simulation of extreme precipitation events by stochastic weather generators. Water Resour. Res. 44 (12).

Hartigan, J.A., Wong, M.A., 1979. Algorithm AS 136: A k-means clustering algorithm. J. R. Stat. Soc. Ser. C (Applied Statistics) 28 (1), 100–108.

Hersbach, H., Bell, B., Berrisford, P., Hirahara, S., Horányi, A., Muñoz-Sabater, J., Nicolas, J., Peubey, C., Radu, R., Schepers, D., et al., 2020. The ERA5 global reanalysis. Q. J. R. Meteorol. Soc. 146 (730), 1999–2049.

Huizinga, J., De Moel, H., Szewczyk, W., 2017. Global flood depth-damage functions: Methodology and the database with guidelines. Tech. rep., Joint Research Centre.

Iacomino, C., Pascale, S., Zappa, G., Iotti, M., Grazzini, F., Ghinassi, P., Portal, A., 2025. A classification of high-risk atmospheric circulation patterns for Italian precipitation extremes. Int. J. Climatol. e70118.

IPCC, W.G.I..I., 2012. Managing the Risks of Extreme Events and Disasters to Advance Climate Change Adaptation. Tech. rep., Intergovernmental Panel on Climate Change (IPCC), p. 582, A Special Report of Working Groups I and II, Cambridge University Press.

Johnson, S.J., Stockdale, T.N., Ferranti, L., Balmaseda, M.A., Molteni, F., Magnusson, L., Tietsche, S., Decremer, D., Weisheimer, A., Balsamo, G., et al., 2019. Seas5: the new ecmwf seasonal forecast system. Geoscientific Model Development 12 (3), 1087–1117.

Kam, P.M., Cache, T., Biess, B., Lohrey, S., di Vincenzo, S., McCaughey, J.W., Horton, R., Thalheimer, L., 2025. Advancing human displacement modelling: A case study of the 2022 summer floods in Pakistan. Authorea Prepr..

Kelder, T., Heinrich, D., Klok, L., Thompson, V., Goulart, H.M., Hawkins, E., Slater, L.J., Suarez-Gutierrez, L., Wilby, R.L., Coughlan de Perez, E., et al., 2025. How to stop being surprised by unprecedented weather. Nat. Commun. 16 (1), 2382.

Kelder, T., Marjoribanks, T., Slater, L., Prudhomme, C., Wilby, R., Wagemann, J., Dunstone, N., 2022a. An open workflow to gain insights about low-likelihood high-impact weather events from initialized predictions. Meteorol. Appl. 29 (3), e2065.

Kelder, T., Müller, M., Slater, L., Marjoribanks, T., Wilby, R., Prudhomme, C., Bohlinger, P., Ferranti, L., Nipen, T., 2020. Using UNSEEN trends to detect decadal changes in 100-year precipitation extremes. Npj Clim. Atmospheric Sci. 3 (1), 47.

Kelder, T., Wanders, N., van der Wiel, K., Marjoribanks, T., Slater, L.J., l Wilby, R., Prudhomme, C., 2022b. Interpreting extreme climate impacts from large ensemble simulations—are they unseen or unrealistic? Environ. Res. Lett. 17 (4), 044052.

Kent, C., Dunstone, N., Tucker, S., Scaife, A.A., Brown, S., Kendon, E.J., Smith, D., McLean, L., Greenwood, S., 2022. Estimating unprecedented extremes in UK summer daily rainfall. Environ. Res. Lett. 17 (1), 014041.

Kent, C., Pope, E., Dunstone, N., Scaife, A.A., Tian, Z., Clark, R., Zhang, L., Davie, J., Lewis, K., 2019. Maize drought hazard in the northeast farming region of China: unprecedented events in the current climate. J. Appl. Meteorol. Clim. 58 (10), 2247–2258.

Kent, C., Pope, E., Thompson, V., Lewis, K., Scaife, A.A., Dunstone, N., 2017. Using climate model simulations to assess the current climate risk to maize production. Environ. Res. Lett. 12 (5), 054012.

Kimutai, J., Vautard, R., Zachariah, M., Tolasz, R., Šustková, V., Cassou, C., Skalák, P., Clarke, B., Haslinger, K., Vahlberg, M., et al., 2024. Climate change and high exposure increased costs and disruption to lives and livelihoods from flooding associated with exceptionally heavy rainfall in central europe.

Klehmet, K., Berg, P., Bozhinova, D., Crochemore, L., Du, Y., Pechlivanidis, I., Photiadou, C., Yang, W., 2024. Robustness of hydrometeorological extremes in surrogated seasonal forecasts. Int. J. Climatol. 44 (5), 1725–1738.

Lang, A., Poschlod, B., 2024. Updating catastrophe models to today's climate–an application of a large ensemble approach to extreme rainfall. Clim. Risk Manag. 44, 100594.

Lehner, B., Verdin, K., Jarvis, A., 2008. New global hydrography derived from spaceborne elevation data. Eos, Trans. Am. Geophys. Union 89 (10), 93–94.

Llasat, M.C., 2024. Spain's flash floods reveal a desperate need for improved mitigation efforts. Nature 635 (8040), 787.

Macdonald, E., Merz, B., Nguyen, V.D., Vorogushyn, S., 2025. Heavy-tailed flood peak distributions: what is the effect of the spatial variability of rainfall and runoff generation? Hydrol. Earth Syst. Sci. 29, 447–463. http://dx.doi.org/10.5194/hess-29-447-2025.

Marchi, M., Bertolini, I., Tonni, L., Morreale, L., Colombo, A., Simonelli, T., Gottardi, G., 2025. An extensive Italian database of river embankment breaches and damages. Water 17 (15), 2202.

Martins, E.S., Stedinger, J.R., 2000. Generalized maximum-likelihood generalized extreme-value quantile estimators for hydrologic data. Water Resour. Res. 36 (3), 737–744. http://dx.doi.org/10.1029/1999WR900330.

Merz, B., Nguyen, V.D., Guse, B., Han, L., Guan, X., Rakovec, O., Samaniego, L., Ahrens, B., Vorogushyn, S., 2024. Spatial counterfactuals to explore disastrous flooding. Environ. Res. Lett. 19 (4), 044022.

Mohr, S., Ehret, U., Kunz, M., Ludwig, P., Caldas-Alvarez, A., Daniell, J.E., Ehmele, F., Feldmann, H., Franca, M.J., Gattke, C., et al., 2022. A multi-disciplinary analysis of the exceptional flood event of july 2021 in central europe. Part 1: Event description and analysis. Nat. Hazards Earth Syst. Sci. Discuss. 2022, 1–44.

Ng, K.S., Leckebusch, G.C., 2021. A new view on the risk of typhoon occurrence in the western north Pacific. Nat. Hazards Earth Syst. Sci. 21 (2), 663–682. http://dx.doi.org/10.5194/nhess-21-663-2021.

Osinski, R., Lorenz, P., Kruschke, T., Voigt, M., Ulbrich, U., Leckebusch, G., Faust, E., Hofherr, T., Majewski, D., 2016. An approach to build an event set of European windstorms based on ecmwf EPS. Nat. Hazards Earth Syst. Sci. 16 (1), 255–268.

Paprotny, D., Rhein, B., Vousdoukas, M.I., Terefenko, P., Dottori, F., Treu, S., Śledziowski, J., Feyen, L., Kreibich, H., 2024a. Merging modelled and reported flood impacts in europe in a combined flood event catalogue for 1950–2020. Hydrol. Earth Syst. Sci. 28 (17), 3983–4010.

Paprotny, D., 't Hart, C.M.P., Morales-Nápoles, O., 2025. Evolution of flood protection levels and flood vulnerability in europe since 1950 estimated with vine-copula models. Natural Hazards 121 (5), 6155–6184.

Paprotny, D., Terefenko, P., Śledziowski, J., 2024b. HANZE v2. 1: an improved database of flood impacts in europe from 1870 to 2020. Earth Syst. Sci. Data 16 (11), 5145–5170.

Pascale, S., Kapnick, S.B., Delworth, T.L., Cooke, W.F., 2020. Increasing risk of another cape town "day zero" drought in the 21st century. Proc. Natl. Acad. Sci. 117 (47), 29495–29503.

Pearl, J., 2009. Causal inference in statistics: An overview.

Perkins-Kirkpatrick, S.E., Stone, D.A., Mitchell, D.M., Rosier, S., King, A.D., Lo, Y.T.E., Pastor-Paz, J., Frame, D., Wehner, M., 2022. On the attribution of the impacts of extreme weather events to anthropogenic climate change. Environ. Res. Lett. 17 (2), 024009.

Philip, S., Kew, S., van Oldenborgh, G.J., Otto, F., Vautard, R., van Der Wiel, K., King, A., Lott, F., Arrighi, J., Singh, R., et al., 2020. A protocol for probabilistic extreme event attribution analyses. Adv. Stat. Clim. Meteorol. Ocean. 6 (2), 177–203.

Poschlod, B., Willkofer, F., Ludwig, R., 2020. Impact of climate change on the hydrological regimes in bavaria. Water 12 (6), 1599. http://dx.doi.org/10.3390/w12061599.

Renard, B., Lang, M., 2007. Use of a Gaussian copula for multivariate extreme value analysis: Some case studies in hydrology. Adv. Water Resour. 30 (4), 897–912. http://dx.doi.org/10.1016/j.advwatres.2006.08.001.

Rhein, B., Kreibich, H., 2025. Causes of the exceptionally high number of fatalities in the ahr valley, Germany, during the 2021 flood. Nat. Hazards Earth Syst. Sci. 25 (2), 581–589.

Riedel, L., Röösli, T., Vogt, T., Bresch, D.N., 2024. Fluvial flood inundation and socio-economic impact model based on open data. Geosci. Model. Dev. 17 (13), 5291–5308.

Rodrigues, R.R., Shepherd, T.G., 2022. Small is beautiful: climate-change science as if people mattered. PNAS Nexus 1 (1), pgac009.

Román, M.O., Wang, Z., Sun, Q., Kalb, V., Miller, S.D., Molthan, A., Schultz, L., Bell, J., Stokes, E.C., Pandey, B., et al., 2018. Nasa's black marble nighttime lights product suite. Remote Sens. Environ. 210, 113–143.

Röösli, T., Appenzeller, C., Bresch, D.N., 2021. Towards operational impact forecasting of building damage from winter windstorms in Switzerland. Meteorol. Appl. 28 (6), e2035.

Sauer, I.J., Reese, R., Otto, C., Geiger, T., Willner, S.N., Guillod, B.P., Bresch, D.N., Frieler, K., 2021. Climate signals in river flood damages emerge under sound regional disaggregation. Nat. Commun. 12 (1), 2128.

Schaller, N., Sillmann, J., Müller, M., Haarsma, R., Hazeleger, W., Hegdahl, T.J., Kelder, T., van den Oord, G., Weerts, A., Whan, K., 2020. The role of spatial and temporal model resolution in a flood event storyline approach in western Norway. Weather. Clim. Extrem. 29, 100259.

Scussolini, P., Aerts, J.C., Jongman, B., Bouwer, L.M., Winsemius, H.C., de Moel, H., Ward, P.J., 2016. FLOPROS: an evolving global database of flood protection standards. Nat. Hazards Earth Syst. Sci. 16 (5), 1049–1061.

Shah, M.A.R., Xu, J., Carisi, F., De Paola, F., Di Sabatino, S., Domeneghetti, A., Gerundo, C., Gonzalez-Ollauri, A., Nadim, F., Petruccelli, N., et al., 2023. Quantifying the effects of nature-based solutions in reducing risks from hydrometeorological hazards: Examples from europe. Int. J. Disaster Risk Reduct. 93, 103771.

Sharma, S., Gomez, M., Keller, K., Nicholas, R.E., Mejia, A., 2021. Regional flood risk projections under climate change. J. Hydrometeorol. 22 (9), 2259–2274.

Shepherd, T.G., 2019. Storyline approach to the construction of regional climate change information. Proc. R. Soc. A 475 (2225), 20190013.

Shepherd, T.G., Shepherd, S.J., et al., 2018. Storylines: an alternative approach to representing uncertainty in physical aspects of climate change. Clim. Change 151, 555–571. http://dx.doi.org/10.1007/s10584-018-2317-9.

Sillmann, J., Shepherd, T.G., van den Hurk, B., Hazeleger, W., Martius, O., Slingo, J., Zscheischler, J., 2021. Event-based storylines to address climate risk. Earth's Futur. 9, http://dx.doi.org/10.1029/2020EF001783, e2020EF001783.

Stockdale, T., Balmaseda, M., Johnson, S., Ferranti, L., Molteni, F., Magnusson, L., Tietsche, S., Vitart, F., Decremer, D., Weisheimer, A., Roberts, C., Balsamo, G., Keeley, S., Mogensen, K., Zuo, H., Mayer, M., Monge-Sanz, B., 2018. SEAS5 and the future evolution of the long-range forecast system. Technical Memorandum 835, European Centre for Medium-Range Weather Forecasts (ECMWF), Reading, Berkshire, UK, Presented to the Scientific Advisory Committee, October 2018.

Thielen, J., Bartholmes, J., Ramos, M.-H., de Roo, A., 2009. The European flood alert system – part 1: Concept and development. Hydrol. Earth Syst. Sci. 13 (2), 125–140. http://dx.doi.org/10.5194/hess-13-125-2009.

Thiemig, V., Gomes, G.N., Skøien, J.O., Ziese, M., Rauthe-Schöch, A., Rustemeier, E., Rehfeldt, K., Walawender, J.P., Kolbe, C., Pichon, D., et al., 2022. EMO-5: a high-resolution multi-variable gridded meteorological dataset for europe. Earth Syst. Sci. Data 14 (7), 3249–3272.

Thompson, V., Coumou, D., Beyerle, U., Ommer, J., Cloke, H.L., Fischer, E., 2025. Alternative rainfall storylines for the western European july 2021 floods from ensemble boosting. Commun. Earth & Environ. 6 (1), 427.

Thompson, V., Dunstone, N.J., Scaife, A.A., Smith, D.M., Hardiman, S.C., Ren, H.-L., Lu, B., Belcher, S.E., 2019. Risk and dynamics of unprecedented hot months in south east China. Clim. Dyn. 52, 2585–2596.

Thompson, V., Dunstone, N.J., Scaife, A.A., Smith, D.M., Slingo, J.M., Brown, S., Belcher, S.E., 2017. High risk of unprecedented UK rainfall in the current climate. Nat. Commun. 8 (1), 107.

Tradowsky, J.S., Philip, S.Y., Kreienkamp, F., Kew, S.F., Lorenz, P., Arrighi, J., Bettmann, T., Caluwaerts, S., Chan, S.C., De Cruz, L., et al., 2023. Attribution of the heavy rainfall events leading to severe flooding in western europe during july 2021. Clim. Change 176 (7), 90.

Tramblay, Y., Arnaud, P., Artigue, G., Lang, M., Paquet, E., Neppel, L., Sauquet, E., 2023. Changes in mediterranean flood processes and seasonality. Hydrol. Earth Syst. Sci. 27 (15), 2973–2987.

Van Der Knijff, J., Younis, J., De Roo, A., 2010. LISFLOOD: a GIS-based distributed model for river basin scale water balance and flood simulation. Int. J. Geogr. Inf. Sci. 24 (2), 189–212.

Van Oldenborgh, G.J., van Der Wiel, K., Kew, S., Philip, S., Otto, F., Vautard, R., King, A., Lott, F., Arrighi, J., Singh, R., et al., 2021. Pathways and pitfalls in extreme event attribution. Clim. Change 166 (1), 13.

Walz, M.A., Leckebusch, G.C., 2019. Loss potentials based on an ensemble forecast: How likely are winter windstorm losses similar to 1990? Atmospheric Sci. Lett. 20 (4), e891.

Wasko, C., Nathan, R., 2019. Influence of changes in rainfall and soil moisture on trends in flooding. J. Hydrol. 575, 432–441.

van der Wiel, K., Wanders, N., Selten, F., Bierkens, M., 2019. Added value of large ensemble simulations for assessing extreme river discharge in a 2 °C warmer world. Geophys. Res. Lett. 46 (4), 2093–2102. http://dx.doi.org/10.1029/2019GL081967.

Winter, B., Schneeberger, K., Förster, K., Vorogushyn, S., 2020. Event generation for probabilistic flood risk modelling: multi-site peak flow dependence model vs. weather-generator-based approach. Nat. Hazards Earth Syst. Sci. 20 (6), 1689–1703.

Woo, G., 2019. Downward counterfactual search for extreme events. Front. Earth Sci. 7, 340. http://dx.doi.org/10.3389/feart.2019.00340.

World Bank, 2019. World development indicators. https://databank.worldbank.org/source/world-development-indicators. (Accessed 12 June 2025).

Yamamoto, K., Iga, K., Yamazaki, A., 2024. Mergers as the maintenance mechanism of cutoff lows: A case study over europe in july 2021. Mon. Weather Rev. 152 (6), 1241–1256.

Zappa, G., Shepherd, T.G., 2017. Storylines of atmospheric circulation change for European regional climate impact assessment. J. Clim. 30 (16), 6561–6577.

Zeder, J., Sippel, S., Pasche, O.C., Engelke, S., Fischer, E.M., 2023. The effect of a short observational record on the statistics of temperature extremes. Geophys. Res. Lett. 50 (16), e2023GL104090.

Zscheischler, J., Westra, S., Van Den Hurk, B.J., Seneviratne, S.I., Ward, P.J., Pitman, A., AghaKouchak, A., Bresch, D.N., Leonard, M., Wahl, T., et al., 2018. Future climate risk from compound events. Nat. Clim. Chang. 8 (6), 469–477.